doi:10.1038/nature11715

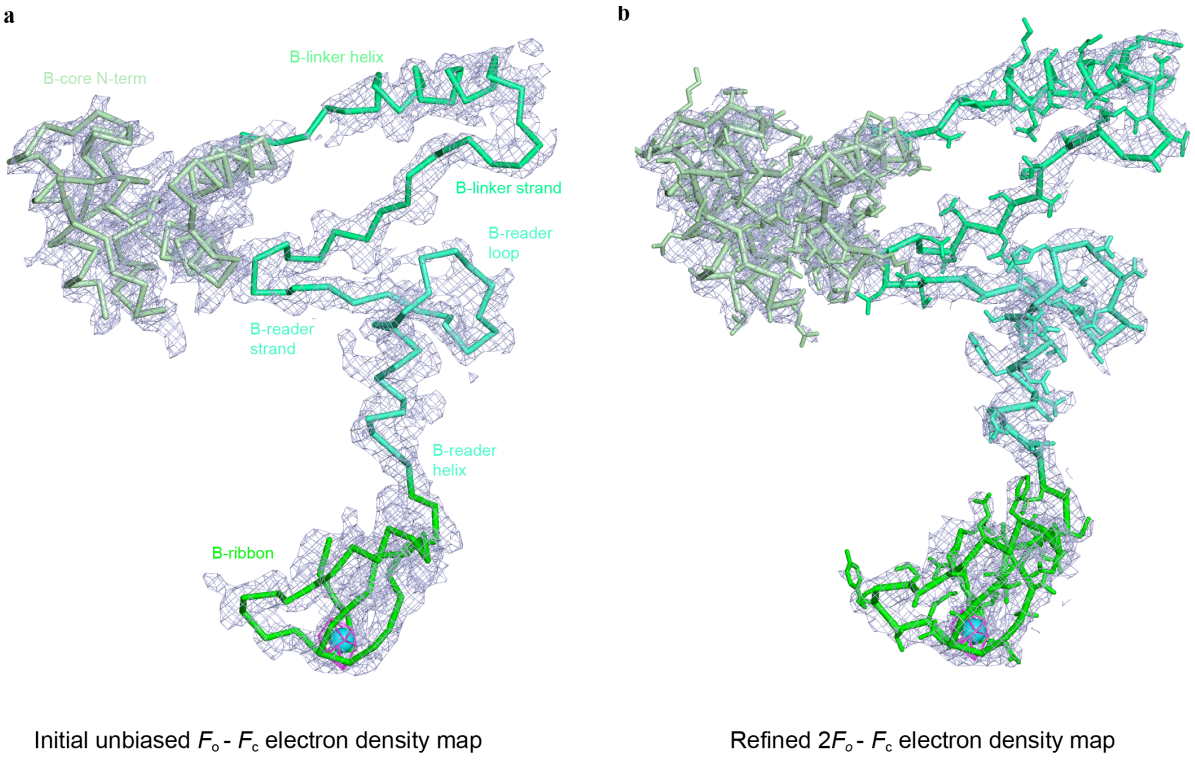

Supplementary Figure 1. Electron density maps for TFIIB in the Pol II-TFIIB complex.
a. Unbiased initial BUSTER mFo-DFc difference electron density map at 2.5 σ (grey mesh) after molecular replacement with the free Pol II structure (1WCM) and refinement with a Pol II structure alone (3HOU without nucleic acids). An anomolous difference Fourier peak at 4 σ (magenta mesh) indicates the position of the zinc atom. A backbone model of the final TFIIB structure is superimposed.
b. Refined BUSTER 2mFo-DFc electron density map contoured at 1 σ (grey mesh). The final TFIIB structure is superimposed and side chains are depicted.

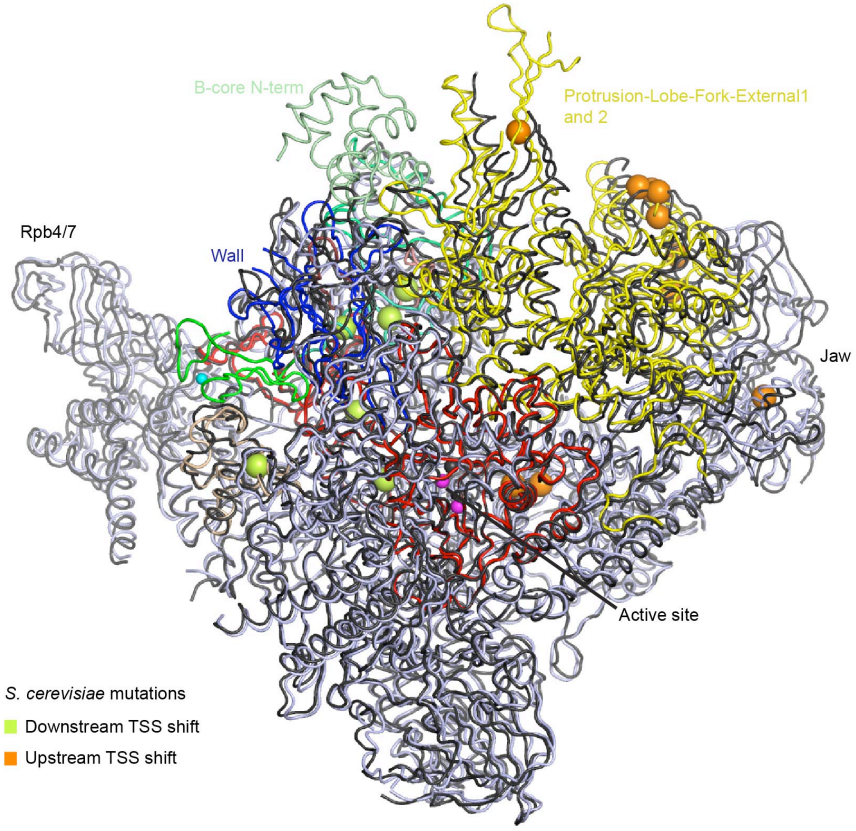

Supplementary Figure 2. TFIIB induces structural changes in Pol II. Overview of TFIIB-induced Pol II domain movements. Structures of the Pol II-TFIIB complex (colours) and free Pol II[10] (dark grey) were superimposed with their Rpb1 subunits.

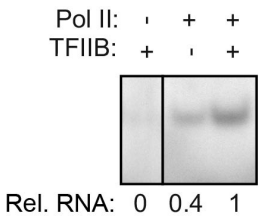

Supplementary Figure 3. TFIIB alone stimulates *de novo* RNA synthesis from the *HIS4* tailed template at near physiological NTP concentration. 500 μM rCTP, rGTP and rUTP, and 50 μM rATP supplemented with 5 μCi [α -^{32}P] rATP was incubated with 2.5 pmol Pol II, 25 pmol TFIIB and 5 pmol of template for 5 min at 301K.

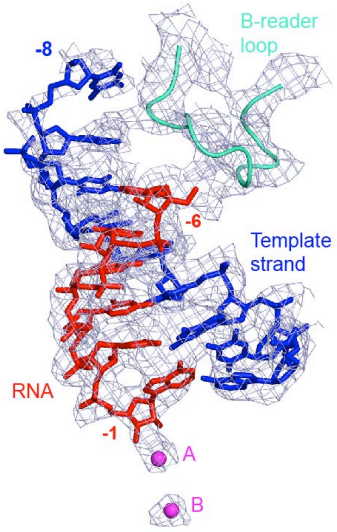

Supplementary Figure 4. Initial unbiased difference electron density for the B-reader loop contoured at 2 σ, DNA-RNA hybrid, and active site metal ions.

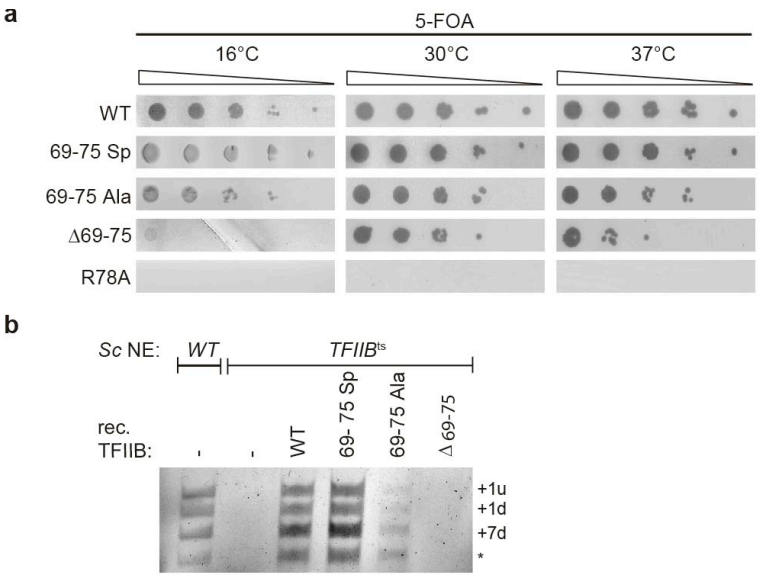

Supplementary Figure 5. Functional analysis of B-reader loop and TFIIB-stimulated RNA chain initiation. a, B-reader loop is required for normal cell growth at non-optimal temperatures. Yeast complementation assay with selection on 5-fluoroorotic acid (5-FOA). **b**, B-reader loop is required for promoter- and activator-dependent transcription *in vitro*. Transcriptional activity from a *HIS4-SNR14* fusion promoter template using a nuclear extract from a strain carrying a temperature-sensitive TFIIB mutation (*TFIIB*^{ts}) is restored upon addition of recombinant wild-type TFIIB (WT) or a TFIIB variant carrying the B-reader loop residues 69-75 from *S. pombe* (69-75 Sp). TSS sites are indicated on the right[1]. TFIIB variants that either lack residues 69-75 (Δ69-75) or carry alanine mutations of these residues (69-75 Ala) do not restore activity.

Supplementary Table 1. Data collection and refinement statistics

	Pol II-TFIIB complex	ITC (Pol II-TFIIB with DNA and 6 nt RNA)
Data collection[a]		
Space group	$C222_1$	$C222_1$
Cell dimensions		
a, *b*, *c* (Å)	222.4, 386.8, 254.4[b]	222.2, 386.0, 254.5
α, β, γ (°)	90, 90, 90	90, 90, 90
Resolution (Å)	50-3.4 (3.50-3.4)[c]	50-3.6 (3.69-3.6)
R_{svm}	38.5 (178.4)	23.3 (115.0)
$I/\sigma I$	7.8 (1.7)	9.5 (2.2)
Completeness (%)	99.9 (99.7)	99.9 (100.0)
Redundancy	7.7 (7.5)	7.5 (7.7)
$CC_{(1/2)}$[d] (%)	97.6 (51.9)	99.2 (73.1)
Refinement		
Resolution (Å)	50-3.4	50-3.6
No. reflections	149749	125981
R_{work}/ R_{free}	17.5/21.1[e]	18.5/22.5[f]
No. atoms		
Protein	32789	32797
Ligand/ion	11	623
Water	0	0
B-factors		
Protein	75.6	106.3
Ligand/ion	76.2	208.1
Water	-	-
R.m.s deviations		
Bond lengths (Å)	0.010	0.08
Bond angles (°)	1.33	1.12
Zn peak for TFIIB in anomalous Fourier [σ][g]	5.8	5.4
Ramachandran[h]		
Preferred/allowed/disallowed (%)	90.8/7.0/2.2	91.5/6.8/1.7

[a]Diffraction data were collected at beamline X06SA of the Swiss Light Source, Switzerland and processed with XDS[35].

[b]Free Pol II $C222_1$ unit cell ≈ 222, 393, 282.

[c]Numbers in parenthesis refer to the highest resolution shell.

[d]$CC_{1/2}$ = percentage of correlation between intensities from random half-datasets[36].

[e]Structure determined from a single crystal using molecular replacement with MOLREP[37] using 12 subunit Pol II alone (1WCM) and refined with BUSTER (Global Phasing Limited).

[f]Structure determined from a single crystal and refined with PHENIX[38].

[g]Calculated at 7 Å resolution using phases from Pol II alone after initial refinement.

[h]Calculated with MolProbity[39].

References

35 Kabsch, W. Xds. *Acta crystallographica. Section D, Biological crystallography* **66**, 125-132, doi:10.1107/S0907444909047337 (2010).

36 Karplus, P. A. & Diederichs, K. Linking crystallographic model and data quality. *Science* **336**, 1030-1033, doi:10.1126/science.1218231 (2012).

37 Vagin, A. & Teplyakov, A. An approach to multi-copy search in molecular replacement. *Acta crystallographica. Section D, Biological crystallography* **56**, 1622-1624 (2000).

38 Adams, P. D. *et al*. PHENIX: a comprehensive Python-based system for macromolecular structure solution. *Acta crystallographica. Section D, Biological crystallography* **66**, 213-221, doi:10.1107/S0907444909052925 (2010).

39 Davis, I. W. *et al*. MolProbity: all-atom contacts and structure validation for proteins and nucleic acids. *Nucleic acids research* **35**, W375-383, doi:10.1093/nar/gkm216 (2007).